

Efficient estimation method for State of Charge of multi-cell battery pack considering cell inconsistency

Zhigang He¹, Yingjie Jin^{1,*}, Shuai Hu², Wei-quan Li³, Xiang-gang Zhang¹

¹ College of Automotive and Traffic Engineering, Jiangsu University, Jiangsu Province, Zhenjiang 212013, China.

² Yongkang Quality and Technology Monitoring Institute (national inspection center for Hardware & Door Product Quality (Zhejiang)), Zhejiang ,321300, China.

³ Zhejiang Fangyuan Test Group Co. Ltd, Zhejiang 310018, China.

*E-mail: 798125859@qq.com

Received: 3 May 2022 / Accepted: 9 June 2022 / Published: 4 July 2022

State of charge (SOC) is an important state quantity for the normal operation of lithium batteries in electric vehicle. At present, SOC estimation research mainly focuses on single cell, and few papers study the SOC of each cell in the battery pack, which gives the capacity estimation of the battery, and SOH estimation, as well as battery equalization bring technical difficulties and even safety issues. However, it is difficult to conduct the SOC estimation of multiple cells in a battery pack due to the inconsistency, which leads to very complex modeling and algorithms. Aiming at the above problems, this paper proposes a low computational multi-cell SOC estimation method. First, for the series battery pack, the capacity, ohmic resistance and voltage are selected as the inconsistency factors considered in this study, and a battery pack difference model based on the equivalent circuit model (ECM) is established. Then, the model parameters were identified online using recursive least squares with forgetting factors (FFRLS). On this basis, a dual adaptive extended Kalman filter (Dual-AEKF) algorithm is constructed to estimate the SOC of all cells in the series battery pack. Finally, three representative dynamic working conditions are used to verify the SOC estimation accuracy of the proposed method and the robustness of the algorithm. The verification results show that the proposed method can significantly reduce the estimation time on the premise of ensuring the accuracy of cell SOC estimation and the robustness of the algorithm.

Keywords: SOC estimation, Lithium-ion battery pack, Cell inconsistency, Dual-AEKF, Efficient Algorithm

1. INTRODUCTION

At the same time that electric vehicles are booming, accidents of battery packs catching fire frequently occur. In order to suppress or even eradicate the occurrence of this phenomenon, it is

necessary to monitor the operating status of each cell in the battery pack. Then, SOC is the most important state quantity of the battery system [1,2], therefore, it is necessary to estimate the SOC of the cells in the battery pack.

Commonly used SOC estimation methods mainly include the following: (1) Ampere-hour integration method[3]; (2) Open circuit voltage (OCV) method[4]; (3) machine learning method[5]; (4) Kalman filter (KF) algorithm[6]. The first two are traditional estimation methods, among which the ampere-hour integration method is widely used in electric vehicle SOC estimation, but the error of current measurement is inevitable, and the accumulated error caused by this makes the SOC estimation value increasingly inaccurate, so this method is often used in conjunction with the OCV method to eliminate accumulated errors. The OCV method is based on the relationship between the OCV and SOC to obtain the current SOC by looking up the table. The disadvantage is that it requires the battery to stand for a long time to obtain a relatively accurate OCV. Therefore, in practical applications, it is often used for initial correction when the BMS is turned on. or battery end-of-charge correction.

Machine learning method mainly include feed-forward neural network (FNN) [7-10], recurrent neural network (RNN) [11-13], support vector machine (SVM) [14], Gaussian process regression (GPR) [15,16]. There are many types of FNN, including back propagation neural networks (BPNN), extreme machine learning, and deep feedforward neural networks. Ref [7] proposes the improved BPNN, and used the OCV, battery charge and discharge current and internal resistance as input to train the model. In general, no matter what machine learning algorithms are, they are all based on data-driven methods, and various optimization algorithms can never eradicate the shortcomings of the model's strict requirements on data quality and quantity. Therefore, there are still great difficulties in the practical application of SOC estimation methods based on machine learning.

The SOC estimation method based on KF can avoid the above problems. It uses the measured values such as voltage and current to correct the real-time estimated value, and expects to obtain the optimal estimation result [6]. Since the battery is a highly nonlinear system, and the traditional KF method is not suitable for dealing with nonlinear systems, so the extended Kalman filter (EKF) algorithm is introduced to obtain better estimation results [17,18]; In addition, a better SOC estimation algorithm can be obtained by combining two EKF filters. For example, the Dual EKF proposed in Ref [19] that uses two independent EKF to estimate the SOC and battery parameters respectively, which improves the computational efficiency; EKF linearizes nonlinear systems through a first-order Taylor series expansion, which usually leads to higher-order loss errors, while cubature Kalman filter (CKF) [20-22] and unscented Kalman filter (UKF) [23-25] can solve this problem very well. UKF uses unscented transformation for prior state estimation, CKF uses spherical radial volume rule to calculate the posterior mean and variance of nonlinear Bayesian filters. This algorithm has better prediction accuracy for nonlinear systems. Ref [20] proposes an improved SOC estimation method based on CKF, and the verification results show that it has better estimation robustness than the EKF. Ref [23] uses the UKF method to calculate the SOC of lithium-ion batteries in real time, and combines three commonly used ECM to verified that the proposed method has good estimation accuracy and robustness. In addition, the traditional KF algorithm cannot automatically correct the process noise and measurement noise, so various adaptive noise correction methods emerge [26-30]. The method of noise adaptive update can improve the accuracy of battery SOC estimation and improve the robustness of the algorithm, but at the

same time increase the computational burden. The KF family of algorithm has shown good performance in battery SOC estimation. Although the EKF is slightly less accurate, the calculation is relatively simple, so it is more suitable for practical application.

The majority of SOC estimation studies are based on single cell, there are few studies on the estimation of battery pack SOC or multi-cell SOC within a battery pack, especially the battery SOC estimation considering the inconsistency of battery cells. It has more practical engineering application value, but it is more difficult. In Ref [18], a series battery pack model is established based on the second-order RC ECM, and the improved EKF is used to estimate its SOC, in order to reduce the calculation amount, the impedance parameters of all cells considered equal, this method cannot characterize the difference between the cells, and in some cases, the obtained pack SOC is only a vague value. As an improvement, the series pack model was established in Ref [31], the SOC and internal resistance of the specific cell, the remaining cell difference SOC and internal resistance, and the capacity of all battery cells were calculated on a three-level time scale, the error of the entire SOC estimation is within 5%. However, this method can only obtain relatively accurate cell SOC in a short time, as the number of battery cycles increases, the errors continue to accumulate and eventually cannot meet the accuracy requirements. The method of 'representative cell' proposed in Ref [32], and the SOC of each representative cell is estimated based on the recursive least squares- AEKF algorithm. The results show that the method can estimate SOC accurately and with low complexity. The disadvantage of this method is that the selection of representative cells in the battery aging process may increase the SOC estimation error of the battery pack, and the monitoring and management of 'non-representative cells' are lacking. Ref [33-35] believe that the SOC estimation of the battery pack is subject to the maximum and minimum voltage (or maximum and minimum SOC) cells during the charging and discharging process. Ref [33] established the battery pack empirical model of the first overcharged cell and the first over-discharged cell, and used the unscented particle filter (UPF) algorithm to estimate the SOC of the battery pack. In Ref [34], all cells' SOC of battery pack is obtained on two time scales, where the highest and lowest SOC estimations are performed at each sampling interval and used for battery pack SOC estimation, while the SOC estimation of rest cells is mainly used for the cell balance control. In Ref [35], a central difference KF SOC estimation method based on the Thevenin ECM was proposed. The Thevenin model was established for the two cells with the lowest and highest voltage and independent model parameters were identified. The SOC estimation accuracy can be controlled within $\pm 2\%$. Obviously, the SOC estimation method that only considers two battery cells cannot well characterize the SOC of other cells, and it is not convenient for the battery management system (BMS) to monitor the cells in real time. Ref [36], a lumped-parameter ECM of the battery pack is proposed, and the battery pack model with multiple cells connected in series is simplified into an improved Thevenin model by mathematical methods, and the SOC is estimated by using the AEKF. Because this simplification ultimately involves only one ECM, the cells' SOC cannot be obtained, which may cause overcharge or discharge. To sum up, the current research basically aims at estimating the SOC of the battery pack, and lacks the monitoring of the SOC of the cells inside the battery pack.

Accurate battery pack model and cell SOC estimation can monitor the operating state of the battery cells inside the battery pack, provide technical support for the capacity estimation of the battery cell and the battery pack, the calculation of SOH, and the balance control of the battery, and ensure the

battery pack is safe to use. In order to achieve these goals, inconsistency factors such as battery cell voltage, capacity, and impedance must be considered. However, there are currently insufficient studies considering inconsistent. In this paper, a low computational multi-cell SOC estimation method for series-connected battery pack is proposed to solve the problem of oversimplification of inconsistency or complicated calculation in current battery pack SOC estimation research. In order to reflect the inconsistency of the battery cells and achieve the purpose of simplifying the calculation, a battery pack difference model based on the ECM is established, and the model parameters are identified online by FFRLS.

The framework of this paper is as follows: Section 2 summarizes the battery inconsistency and identifies the inconsistency factors that this paper focuses on. Section 3 established a simplified series battery pack difference model for the considered inconsistency factors and conducted online parameter identification. Section 4, proposing a Dual-AEKF algorithm based on the previously established model and parameter identification results. In Section 5, the proposed method is experimentally verified using DST, HPPC and the bus equivalent working conditions. The last section gives the research conclusions.

2. BATTERY INCONSISTENCY

Battery inconsistency is inevitable, which first comes from differences in manufacturing process, precision, and materials[37]. During the battery production process, it is impossible to ensure that the material, coating uniformity and electrode thickness are completely consistent[38,39], which leads to inconsistencies in voltage[40], initial capacity, impedance, and heat generation[41]. In the process of cell usage, the differences in the internal resistance of the connecting sheets of the series battery packs and the different heat dissipation conditions caused by the location of the cells in the battery pack will aggravate the inconsistency.

The battery inconsistencies mainly include: voltage inconsistency, impedance inconsistency, capacity inconsistency and decay rate inconsistency[40], heat generation inconsistency[42]. (called internal inconsistency); External inconsistencies include different cell positions within the pack and differences in the internal resistance of the connecting sheets[43]. First of all, the voltage inconsistency is the most intuitive. The lowest voltage cell directly limits the discharge capacity of the series-connected battery pack. The voltage inconsistency of the battery pack without a balanced system will increase as the battery aging. Secondly, the inconsistency of battery capacity causes different discharge rates of cells in parallel battery packs, and different depths of discharge for cells in series battery packs. Battery impedance parameters, internal resistance of connecting sheets, and battery heat generation and heat transfer (location factor, cooling effect), these factors together cause different capacity decay rates and different power decay rates of cells[41], and further aggravate the inconsistency of battery capacity and battery heat production and heat exchange.

Battery inconsistency is inevitable and increases gradually during battery service. In order to obtain accurate cells' SOC, prevent overcharge and overdischarge of the battery pack, and ensure the safe operation of the battery pack, battery inconsistency must be considered. The inconsistency of the

capacity, ohmic resistance and voltage of the battery cells directly affects the accuracy of SOC estimation, so it is regarded as the focus of this paper.

3. BATTERY PACK DIFFERENCE MODEL AND PARAMETER IDENTIFICATION

In order to accurately estimate the multi-cell SOC in the battery pack, first, it is necessary to establish a battery pack model that reflects the inconsistency of each cell. At present, the commonly used battery models are: electrochemical model, machine learning model and ECM [2,6]. The electrochemical model has many parameters and is too complicated[44], and the machine learning model requires a large amount of data to train the model[16]. In contrast, ECM has the advantages of simple model and easy parameter identification, so this paper takes ECM as the basic unit of battery pack modeling.

3.1 Equivalent circuit model

ECM use circuit elements such as resistors, capacitors, and constant voltage sources to describe battery external characteristics. It has been widely used in SOC estimation. The commonly used ECM include Rint model, Thevenin model, PNGV model and second-order RC ECM. Ref [45] compared the estimation accuracy and stability of SOC under different ECM, and pointed out that the second-order RC ECM has better accuracy and moderate computational complexity. Therefore, this paper adopts the second-order RC ECM shown in Fig 1 as the basis for battery pack modeling.

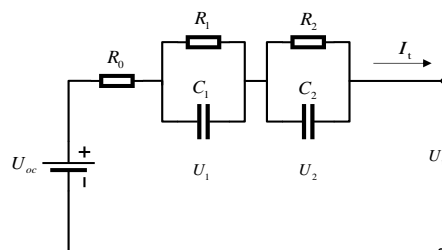


Figure 1. Second-order RC ECM

U_{OC} is the OCV of the battery, R_0 is the ohmic internal resistance, U_t represents the terminal voltage of the battery, I_t is the continuous time working current, U_1 represents the activation polarization voltage (on the R_1C_1 loop), R_1 is the activation polarization resistance, C_1 is the activation polarization capacitance, U_2 represents the concentration polarization voltage, R_2 is the concentration polarization resistance, C_2 is the concentration polarization capacitance. The circuit equation of this model can be obtained from Kirchhoff's law as:

$$\begin{cases} \dot{U}_1 = \frac{I}{C_1} - \frac{U_1}{R_1 C_1} \\ \dot{U}_2 = \frac{I}{C_2} - \frac{U_2}{R_2 C_2} \\ U_t = U_{oc} - U_1 - U_2 - I_t R_0 \end{cases} \quad (1)$$

where \dot{U}_1 represents the first derivative of U_1 . Discretize the state space equation of the second-order RC ECM shown in equation (2), and obtain its discrete time iteration equation as:

$$\begin{cases} U_{1,k} = e^{-\frac{T}{\tau_1}} U_{1,k-1} + (1 - e^{-\frac{T}{\tau_1}}) R_1 I_{k-1} \\ U_{2,k} = e^{-\frac{T}{\tau_2}} U_{2,k-1} + (1 - e^{-\frac{T}{\tau_2}}) R_2 I_{k-1} \\ U_{t,k} = U_{oc,k} - U_{1,k} - I_k R_0 \end{cases} \quad (2)$$

$U_{1,k}$ and $U_{2,k}$ represent the activation polarization voltage and concentration polarization voltage at time k, respectively, $U_{t,k}$ is the battery terminal voltage at time k, $U_{oc,k}$ is the OCV of the battery at time k, I_{k-1} is the current at time k-1, $\tau_1 = R_1 C_1$; $\tau_2 = R_2 C_2$, T is the sampling time interval.

3.2 Battery pack difference model considering inconsistency

The series battery pack model based on the second-order RC ECM is shown in Figure 2, which contains N battery cells in total, and each battery cell is equivalent to a second-order RC ECM., but the model has many parameters and a huge amount of computation.

In this paper, all the cells of the series battery pack are divided into the selected cell (X) and the remaining cells (1, 2,...N-1), where the selected cell is the cell with the largest SOC, and their corresponding ECM unit is shown in Figure 3. The polarization voltage differences of the remaining cells are ignored. In order to reduce the voltage estimation errors of the remaining cells, the calculated value of the polarization voltage of the selected cell at each sampling time are used to compensate the voltage estimate values of the remaining cells (Details are in section 4.3). Under the premise of ensuring the accuracy of the selected cell, the model accuracy errors of the remaining cells are reduced.

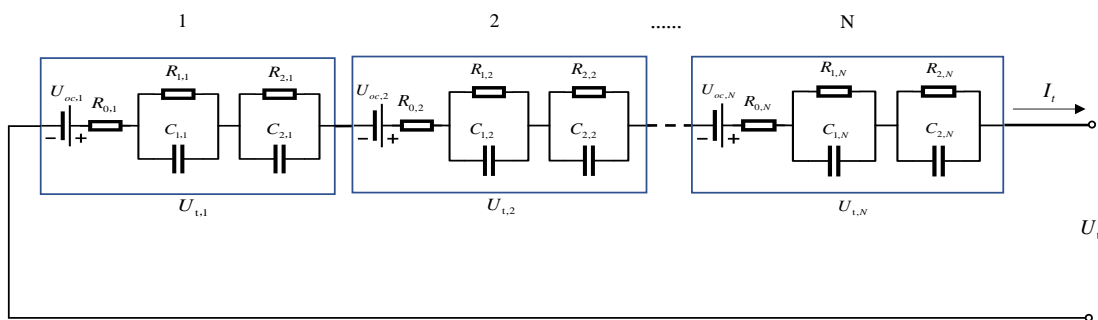


Figure 2. Model of series battery pack based on second-order RC ECM

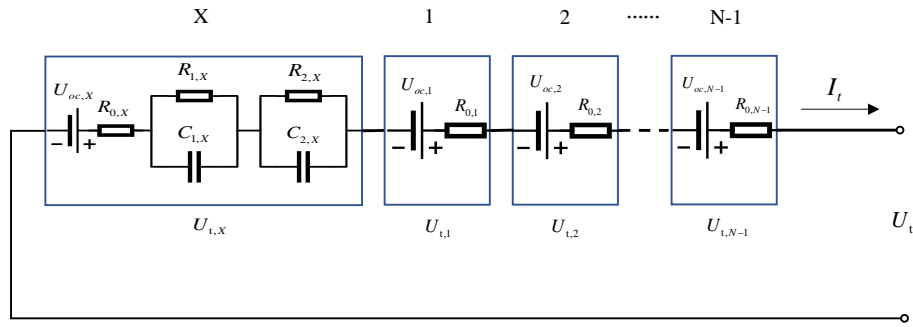


Figure 3. Simplified battery pack difference model

3.3 Parameter identification

Recursive least squares (RLS) has the advantages of easy implementation and fast convergence, FFRLS is introduced in this paper to avoid data saturation and reduce the influence of old data on the identification results[46]. This method is used to online identify the parameters of the battery pack model established in the previous section. The FFRLS derivation process is as follows:

$$z_k = \Phi_k \theta_k \tag{3}$$

z_k denote the observation matrix, Φ_k denote the input and output sequence matrix, and θ_k denote the parameter matrix need to be identified.

By continuously updating z_k and Φ_k , the parameters to be identified at each moment can be identified by the following formula (4).

$$\begin{cases} K_k = P_{k-1} \Phi_k^T [\Phi_k P_{k-1} \Phi_k^T + \lambda]^{-1} \\ \theta_k = \theta_{k-1} + K_k [z_k - \Phi_k \theta_{k-1}] \\ P(k) = \frac{1}{\lambda} P_{k-1} (E - K_k \Phi_k) \end{cases} \tag{4}$$

where K_k and P_k represent the gain matrix and covariance matrix at time k respectively. E is the identity matrix. λ is the forgetting factor, usually between 0.95 and 1.

In order to use FFRLS to identify the parameters of the second-order RC RCM, the equation (1) was discretized, and its Laplace equation is:

$$U_{OC}(s) - U_t(s) = I(s) \left(R_0 + \frac{R_1}{1 + \tau_1 s} + \frac{R_2}{1 + \tau_2 s} \right) \tag{5}$$

Let $s = \frac{2}{T} \frac{1-z^{-1}}{1+z^{-1}}$, the discretized transfer function is available as equation (6).

$$G(z^{-1}) = \frac{a_3 + a_4 z^{-1} + a_5 z^{-2}}{1 - a_1 z^{-1} - a_2 z^{-2}} \tag{6}$$

a_1 、 a_2 、 a_3 、 a_4 、 a_5 are the corresponding constant coefficients, that is, the parameters need to be identified.

According to Equation (6) and further calculation, a new expression of the transfer function will obtain, comparing its relationship with Equation (6), the relationship between the parameter values of the second-order RC ECM and the parameters to be identified can be obtained as follows:

$$\begin{cases} R_0 = \frac{a_3 - a_4 + a_5}{1 + a_1 - a_2}; \\ R_2 = \frac{T \cdot \frac{a_3 - a_5}{1 - a_1 - a_2} - \frac{a_3 - a_4 + a_5}{1 + a_1 - a_2} \cdot l_1 - \frac{a_3 + a_4 + a_5}{1 - a_1 - a_2} \cdot l_2}{t_1 - t_2}; \\ R_1 = \frac{a_3 + a_4 + a_5}{1 - a_1 - a_2} - \frac{a_3 - a_4 + a_5}{1 + a_1 - a_2} - R_2; \\ C_1 = \frac{l_1}{R_1}; \quad C_2 = \frac{l_2}{R_2} \end{cases} \quad (7)$$

Among them:

$$l_1 = \frac{\frac{T(1 + a_2)}{1 - a_1 - a_2} - \sqrt{\frac{T^2(1 + a_2)^2}{(1 - a_1 - a_2)^2} - \frac{T_2(1 + a_1 - a_2)}{1 - a_1 - a_2}}}{2}$$

$$l_2 = \frac{\frac{T(1 + a_2)}{1 - a_1 - a_2} + \sqrt{\frac{T^2(1 + a_2)^2}{(1 - a_1 - a_2)^2} - \frac{T_2(1 + a_1 - a_2)}{1 - a_1 - a_2}}}{2}$$

So far, the parameters of each cell of the battery pack model can be obtained by substituting the identified coefficients a_1 、 a_2 、 a_3 、 a_4 、 a_5 and back into equation (7).

4. BATTERY PACK MULTI-CELL SOC ESTIMATION

4.1 Adaptive extended Kalman Filter algorithm

In the process of SOC estimation using EKF[31], it satisfies the following basic relationship:

$$\begin{cases} x_{k+1} = f(x_k, u_k) + w_k \\ z_k = h(x_k) + v_k \end{cases} \quad (8)$$

Among them $v_k \sim (0, R_k)$, $w_k \sim (0, Q_k)$, where R_k and Q_k represent the measurement noise covariance and process noise covariance respectively, the variables x_{k+1} and z_k represent the state value to be estimated and the measurement value respectively, u_k is the system input (in this paper is I_k).

The battery SOC estimation process based on EKF is the process of correcting the estimated value with the measured value. The specific steps are shown in Table 1:

Table 1. KF algorithm flow:

KF algorithm	
Prior estimation:	$\hat{x}_k^- = F \hat{x}_{k-1}^-$
Prior estimation covariance:	$P_k^- = F P_{k-1}^- F^T + Q_{k-1}$
Measurement equation:	$z_k = H x_k + R_{k-1}$
Revised estimate:	$\hat{x}_k = \hat{x}_k^- + K_k (z_k - H \hat{x}_k^-)$
Update Kalman Gain:	$K_k = P_k^- H^T (H P_k^- H^T + R_{k-1})^{-1}$
Update the posterior	
Estimated covariance:	$P_k = (E - K_k H) P_k^-$

\hat{x}_k^- and \hat{x}_k are the state prior estimation value and state estimation value at time k respectively, F is the system matrix, P_k^- and P_k are the prior estimation covariance and the posterior estimation covariance at time k respectively, \hat{z}_k is the estimated value of the quantity measurement at time k , in this paper that is the estimated value of the battery terminal voltage, K_k is the Kalman gain at time k , H is the state transition matrix, and E is the identity matrix.

In this paper, the Sage-husa adaptive filter is used to update the process noise and measurement noise in the EKF estimation process, so as to form a Dual-AEKF structure. The simplified form in [47] is used:

$$\begin{cases} Q_{k+1} = (1 - d_k)Q_k + d_k(K_{k+1}\varepsilon_k\varepsilon_k^T K_{k+1}^T - P_k^+ + P_k^-) \\ R_{k+1} = (1 - d_k)R_k + d_k\varepsilon_k\varepsilon_k^T \end{cases} \quad (9)$$

Among them, $d_k = (1 - \rho)/(1 - \rho^k)$, ρ is the forgetting factor, generally $\rho \in [0.95 \ 0.99]$, in this paper, take 0.95, $\varepsilon_k = z_k - \hat{z}_k$. z_k is the voltage measurement.

This paper will adopt a dual AEKF structure, in which the first AEKF will be used to calculate the SOC of the selected cell, while the second AEKF will be used to estimate the SOC of the remaining cells, and the parameters of the first AEKF will be sent to the second AEKF to simplify calculation. The establishment process of the key equation of AEKF is given below.

4.2 Selected cell SOC estimation based on AEKF-1

The SOC calculation formula used in this paper is given according to the ampere-hour integration method[3]:

$$SOC(t) = SOC_0 - \frac{\eta}{\eta_T Q_n} \int_{t_0}^t Idt \quad (10)$$

SOC_0 is the initial value of SOC, t is continuous time, η_T is the temperature correction coefficient of the capacity, η is the coulombic efficiency, Q_n is the available capacity of the battery under standard temperature conditions.

Let $Q_N = \eta_T \cdot Q_n$, and discretize the above formula to get equation (11):

$$SOC_k = SOC_{k-1} - \frac{\eta_T}{Q_N} I_{k-1} \quad (11)$$

In the formula, SOC_k represents the battery SOC value at time k . SOC, $U_{1,k}$ and $U_{2,k}$ are selected as state variables, and the calculation method of and has been given by formula (2), and the calculation formula of the state variables of the selected cell is given:

$$\begin{cases} SOC_k = SOC_{k-1} - \frac{\eta_T}{Q_N} I_{k-1} + w_{1,k-1} \\ U_{1,k} = e^{\frac{-T}{\tau_1}} U_{1,k-1} + R_1(1 - e^{\frac{-T}{\tau_1}}) I_{k-1} + w_{2,k-1} \\ U_{2,k} = e^{\frac{-T}{\tau_2}} U_{2,k-1} + R_2(1 - e^{\frac{-T}{\tau_2}}) I_{k-1} + w_{3,k-1} \end{cases} \quad (12)$$

And write the measurement equation according to the second-order RC ECM:

$$U_{t,k,x} = U_{oc,x}(SOC_k) - U_{1,k} - U_{2,k} - R_0 I_k + v_k \quad (13)$$

$U_{t,k,x}$ is the estimated value of the terminal voltage of the selected cell at time k , $U_{oc,x}(SOC_k)$ is the OCV of the battery obtained by looking up the table according to the estimated SOC value of the selected cell at time k .

Write equations (12) and (13) in matrix form, the state equation and measurement equation are:

$$\begin{bmatrix} SOC_k \\ U_{1,k} \\ U_{2,k} \end{bmatrix} = \begin{bmatrix} 1 & 0 & 0 \\ 0 & e^{-\frac{T}{\tau_1}} & 0 \\ 0 & 0 & e^{-\frac{T}{\tau_2}} \end{bmatrix} \times \begin{bmatrix} SOC_{k-1} \\ U_{1,k-1} \\ U_{2,k-1} \end{bmatrix} + I_{k-1} \times \begin{bmatrix} \frac{-\eta T}{Q_N} \\ (1 - e^{-\frac{T}{\tau_1}})R_1 \\ (1 - e^{-\frac{T}{\tau_2}})R_2 \end{bmatrix} + w_{k-1} \quad (14)$$

$$[U_{t,k,x}] = [U_{oc,x}(SOC_k) \quad U_{1,k} \quad U_{2,k}] \begin{bmatrix} SOC_k \\ -1 \\ -1 \end{bmatrix} - [R_0][I_k] + [v_k] \quad (15)$$

4.3 Estimation of the remaining cells' SOC based on AEKF-2

The remaining cells in this paper refer to all battery cells in pack except the selected cell. It can be seen from equation (14) that the state equation of the second-order RC ECM is generally calculated as a three-dimensional matrix. The calculation of the polarization impedance voltage in the state equation is to pave the way for the application in the measurement equation to obtain the estimated value of the battery terminal voltage. In this paper, the calculation of the polarization voltage of the remaining cells is omitted, and the SOC state equation of the remaining cells are simplified as follows:

$$SOC_{k,i} = SOC_{k-1,i} - \frac{\eta T}{Q_{N,i}} \cdot I_{k-1} + w_{k,i} \quad (16)$$

Where $SOC_{k,i}$ represents the SOC of the i-th battery cell at time k, $Q_{N,i}$ represents the capacity of the i-th battery cell; and $w_{k,i}$ represents the system noise distribution of the i-th battery cell at time k, $i=1,2,3... N-1$.

Based on the second-order RC ECM, the measurement equations of the remaining cells are written, such as equations (17) :

$$U_{t,k,i} = U_{OC,k,i} - (U_{1,k,i} + U_{2,k,i}) - I_k R_{0,i} + v_{k,i} \quad (17)$$

$U_{t,k,i}$ represents the terminal voltage of the i-th battery cell at time k. $U_{OC,k,i}$ is the OCV of the remaining cells at time k, $R_{0,i}$ represent the ohmic internal resistance of the i-th battery cell, $U_{1,k,i}$ and $U_{2,k,i}$ represent the activation polarization voltage and concentration polarization voltage of the i-th remaining cell at time k respectively, $v_{k,i}$ represents the measurement noise distribution of the i-th battery cell at time k.

Substitute $U_{1,k,i}$ and $U_{2,k,i}$ with $U_{1,k}$ and $U_{2,k}$, that have been calculated by the equation of state of the selected cell, so that the state and measurement equations of the remaining cells can be obtained as:

$$SOC_{k,i} = SOC_{k-1,i} - \frac{\eta \Delta t}{Q_{N,i}} \cdot I_{k-1} + w_{k,i} \quad (18)$$

$$U_{t,k,i} = U_{OC,k,i} - (U_{1,k} + U_{2,k}) - I_k R_{0,i} + v_{k,i} \quad (19)$$

This simplified method discards the difference in polarization voltage between the remaining cells with selected cell, thereby reducing the three-dimensional calculation of the equation of state to one-dimensional, at the cost of some loss of estimation accuracy, but greatly reducing the calculation the complexity.

The estimation process of the SOC of all cells in the entire battery pack is as Fig 4:

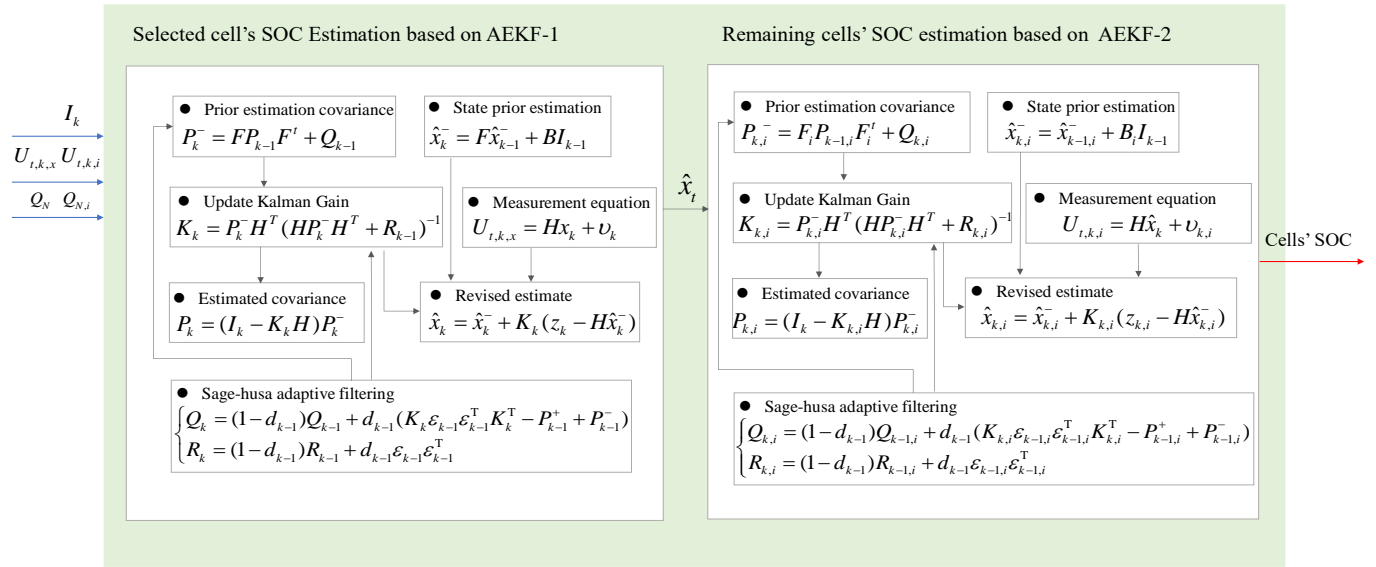


Figure 4. Dual-EKF battery pack multi-cell SOC estimation framework

5. EXPERIMENTAL VERIFICATION

5.1 Experiment introduction

The battery used in this paper is the IMP06160230 ternary lithium-ion soft pack battery, with a nominal capacity of 29Ah. 5 aged batteries were subjected to capacity calibration, OCV test. Their capacities are 27.758Ah, 27.806 Ah, 28.082 Ah, 27.680 Ah, 27.480 Ah respectively. The five battery cells are connected in series to form a battery pack for dynamic stress test (DST), hybrid pulse power characteristic (HPPC) and an equivalent working condition (EWC) test, EWC based on actual operating data of certain pure electric bus. Among them, DST and HPPC can verify the accuracy and algorithm robustness of the proposed SOC estimation method under severe battery discharge conditions, because they simulate battery step discharge, pulse discharge, and short-term high-current discharge (3C discharge) conditions. In addition, in order to be closer to the actual operating conditions of the battery, we collected the operating current of the battery pack of a pure electric bus for a week and established an equivalent working condition. The equivalent process of the current and duration of the EWC is as follow: take 30A as an interval, divide the battery pack discharge current of the pure electric bus by frequency, select the median of the current interval, and then allocate the current duration according to the frequency of current, and finally proportionally reduce the discharge current of the battery pack in this experiment, as shown in Table 2.

Table 2. Current and duration of EWC

Discharge current (A)	duration (S)
3.3	86
9.6	60
3.3	86
28.8	36
3.3	86
35.4	36
3.3	86
54.6	12
3.3	86
58.5	60
3.3	86
48.3	12
3.3	86
41.7	24
3.3	86
22.5	48
3.3	86
16.2	48
3.3	90

The OCV test adopts the discharge-standby method. The OCV-SOC fitting curves of all cells are basically the same, and the OCV-SOC relationship of the selected cell shown in the following figure:

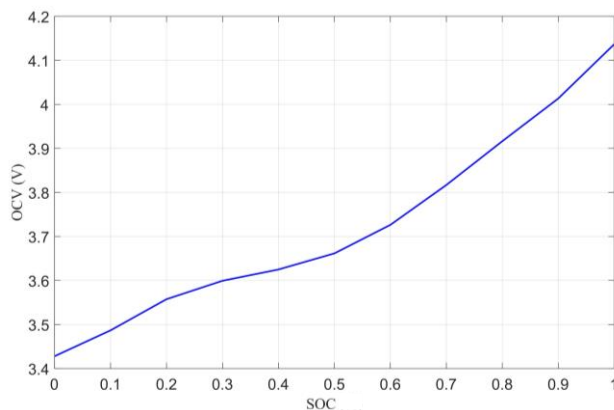


Figure 5. OCV-SOC fitting curve of selected cell

5.2 Verification of dynamic conditions

The selected cell is cell4 in the Figure 6,7,8, and the other cells are cell1, cell2, cell3, and cell5. Figure 6,7,8 shows the estimation results under DST, HPPC, and EWC conditions, respectively. In Figures 6,7,8, (a) and (b) are the SOC estimation results and the error relative to the SOC reference value respectively, they are obtained by the proposed method in this paper (TPM). While (c) and (d) are based

on the method proposed in this paper, but the adaptive filtering method is not used (called: TPM-NA). While (e) and (f) are based on the model in Figure 2, each cell is configured with an independent second-order RC model, the model parameters of each cell are obtained through the parameter identification results. Dual-AEKF algorithm was used to estimate SOC(called: GM)

By comparing the estimation results obtained by TPM and TPM-NA in the three figures, it can be found that the estimation results of the former are better, and the maximum estimation errors of the five cells are significantly reduced. This shows that the Sage-husa adaptive filtering method has a good effect on noise correction.

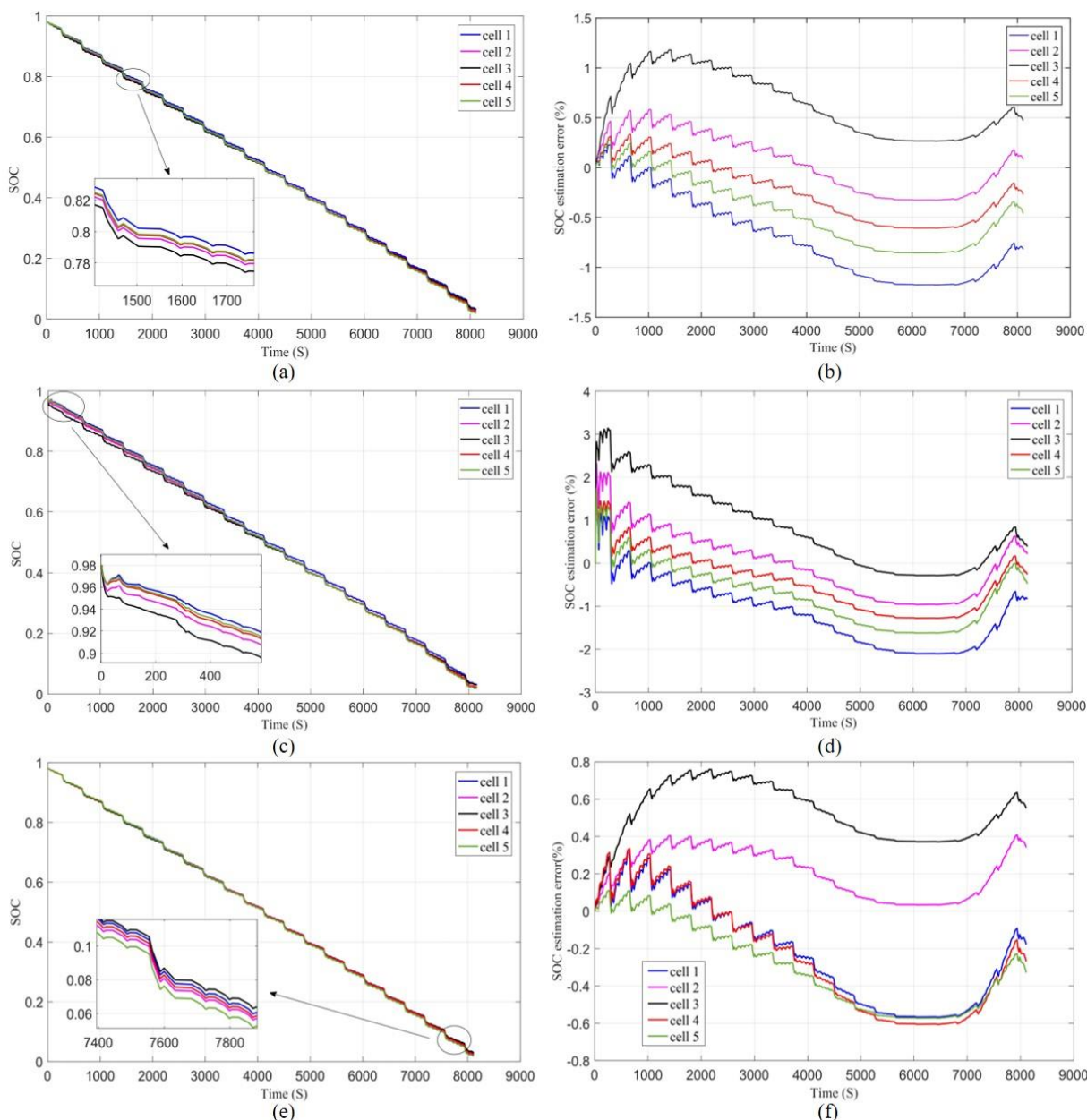


Figure 6. SOC estimation results and errors of cells under DST. (a) SOC estimation results based on TPM; (b) SOC estimation errors based on TPM; (c) SOC estimation results based on TPM-NA; (d) SOC estimation errors based on TPM-NA; (e) SOC estimation results based on GM; (f) SOC estimation errors based on GM.

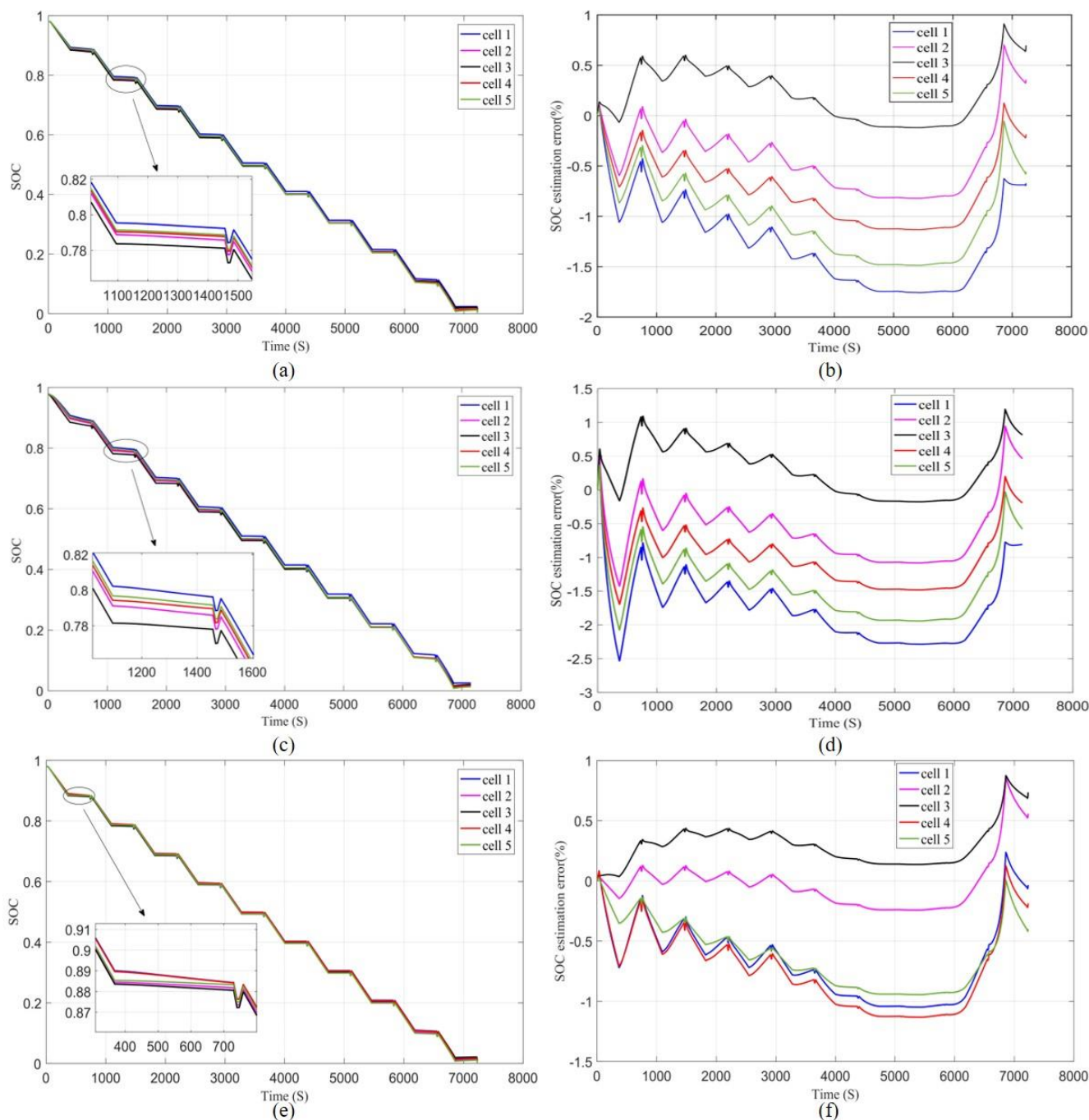


Figure 7. SOC estimation results and errors of cells under HPPC. (a) SOC estimation results based on TPM; (b) SOC estimation errors based on TPM; (c) SOC estimation results based on TPM-NA; (d) SOC estimation errors based on TPM-NA; (e) SOC estimation results based on GM; (f) SOC estimation errors based on GM.

In (f) of the Figure 6,7,8, the error difference between cell1, cell4, and cell5 is small, which indicates that the inconsistency of the three batteries is small. In fact, the voltage, impedance identification data and capacity of the three batteries are really little different. When the polarization impedance parameters of cell4 are used for the rest of the cells, as shown in (b) of Figure 6,7,8, the SOC estimation errors of cell1, cell4, and cell5 are still relatively small. As the battery aging, this difference will not change greatly, because the polarization impedance does not contribute much to the SOC

estimation error[48], and the ohmic internal resistance of the battery mainly affects the SOC estimation accuracy. Therefore, based on TPM, a reliable SOC estimation result can be obtained, and the inconsistency information of the cells (inconsistency degree of battery capacity and voltage) can be obtained from the estimation result.

In a series battery pack, the large error of the single cell may cause inconsistency misjudgment, thus affecting the safe use of the battery, so we should pay more attention to the maximum absolute error of SOC estimation result. In table 3, the maximum SOC estimation errors of the three methods under different working conditions are listed, and the corresponding battery numbers are also given. TPM-based SOC estimation absolute error values under all conditions are below 1.8%. At the same time, the maximum absolute error based on the TPM-NA reaches 3.44%, GM-based SOC absolute error values under all conditions are below 1.13%. The error based on TPM is slightly larger than that based on GM, which is totally acceptable.

Table 4 shows the comparison results of RMSE. In general, the value based on GM is the smallest, while the value based on TPM-NA is the largest, which meet our expectation.

The research goal of this paper is to reduce the amount of calculation under the premise of better accuracy. The above verification shows that the method proposed in this paper can obtain better estimation results. It has been explained in Section 4.2 that TPM reduces the three-dimensional equation of state of the remaining cells to one dimension, thereby reducing the computational burden of the second AEKF. In order to quantify the reduced computational complexity, this paper uses the computer running time to compare the computational complexity of TPM and GM.

Table 3. Maximum SOC estimation error under three working conditions

Dynamic working conditions			
Max error	DST	HPPC	EWC
TPM	1.18%(cell3)	-1.76%(cell1)	1.73%(cell3)
TPM-NA	3.14%(cell3)	-2.53%(cell1)	3.44%(cell3)
GM	0.76%(cell3)	-1.13%(cell4)	0.95%(cell3)

Table 4. RMSE error under different working conditions

		Cell				
	Error	Cell1	Cell2	Cell3	Cell4	Cell5
DST	TPM	0.0101	0.0024	0.0013	0.0072	0.0082
	TPM-NA	0.0132	0.0040	0.0033	0.0092	0.0112
	GM	0.0053	0.0007	0.0023	0.0072	0.0072
HPPC	TPM	0.0071	0.0042	0.0073	0.0022	0.0064
	TPM-NA	0.0084	0.0044	0.0083	0.0023	0.0068
	GM	0.0003	0.0035	0.0065	0.0022	0.0051
EWC	TPM	0.0020	0.0080	0.0110	0.0031	0.0011
	TPM-NA	0.0024	0.0112	0.0132	0.0074	0.0036
	GM	0.0039	0.0077	0.0094	0.0031	0.0003

The results are shown in Table 5. Under the same CPU and memory occupancy rate on the same computer, run the program three times, and fill in the table with the average of the program running time. Under DST, HPPC and EWC, TPM saves time by 48.3%, 35.5%, and 40.6% respectively. Therefore, TPM can reduce the computational complexity under the premise of ensuring a certain accuracy.

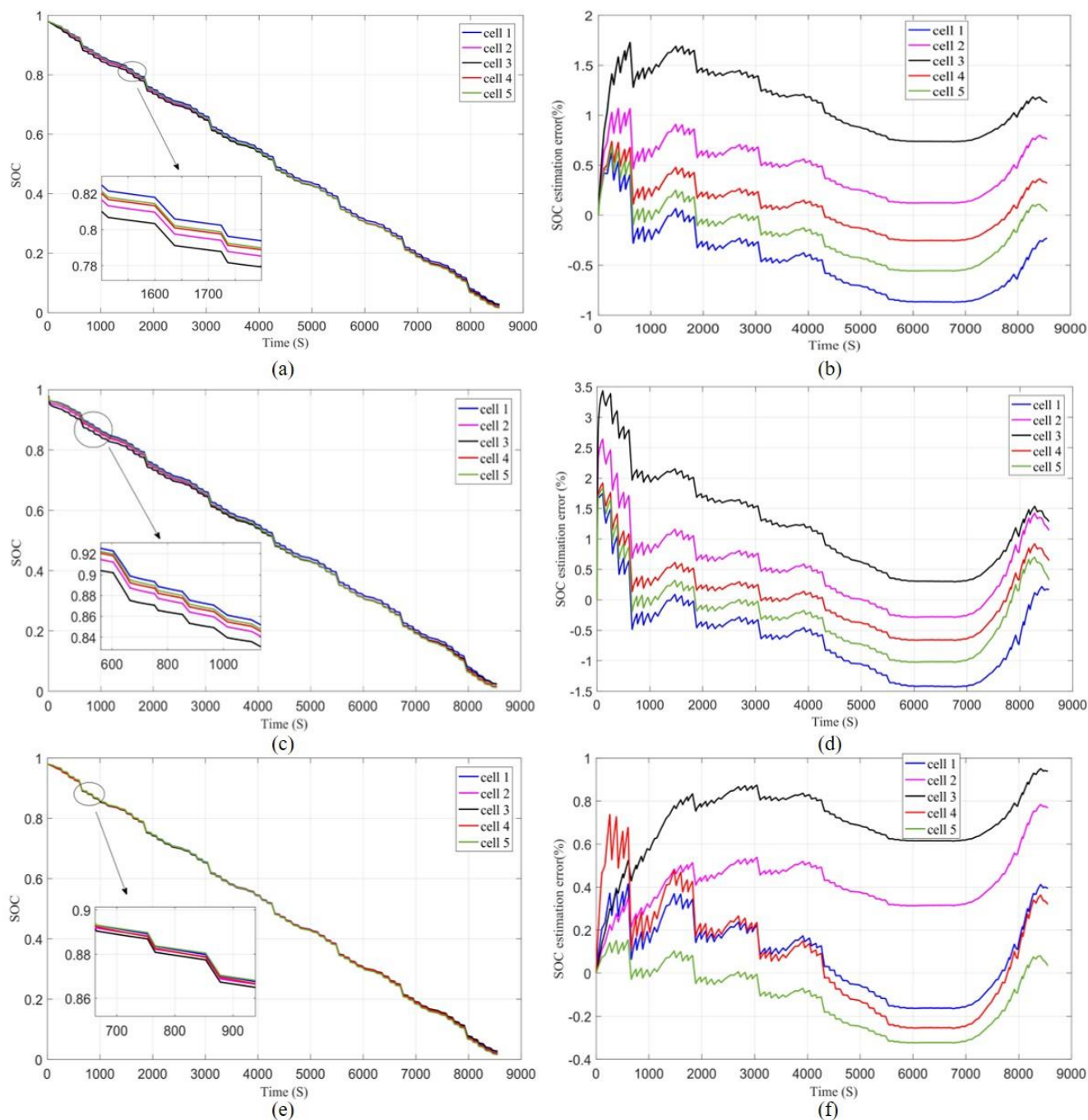


Figure 8. SOC estimation results and errors of cells under EWC. (a) SOC estimation results based on TPM; (b) SOC estimation errors based on TPM; (c) SOC estimation results based on TPM-NA; (d) SOC estimation errors based on TPM-NA; (e) SOC estimation results based on GM; (f) SOC estimation errors based on GM.

It has been explained in Section 4.2 that the efficient method in this paper reduces the three-dimensional equation of state of the remaining cells to one dimension, thereby reducing the computational burden of the second AEKF. In order to quantify the reduced computational complexity, this paper uses the computer running time to compare the computational complexity of the efficient method and the general method. The results are shown in Table 6. Under the same CPU and memory occupancy rate on the same computer, run the program three times, and fill in the table with the average of the program running time. Under DST, HPPC and EWC, TPM saves time by 48.3%, 35.5%, and 40.6% respectively. Therefore, TPM can reduce the computational complexity under the premise of ensuring a certain accuracy.

Table 5. Comparison of the algorithm running time of TPM and GM under various conditions

Dynamic working conditions			
Method	DST	HPPC	EWC
TPM	2.9s	3.1 s	3.2 s
GM	4.3s	4.2 s	4.5 s

In order to verify the robustness of the algorithm, the initial SOC_s of cell1, cell2, cell3, cell4, and cell5 are set to 90%, 80%, 70%, 60%, and 50% respectively, and the cell SOC is estimated under DST conditions, as shown in Figure 9(a), (b), around 1000 seconds, the SOC estimation errors of all cells recover to a small value, indicating that the algorithm has better robustness.

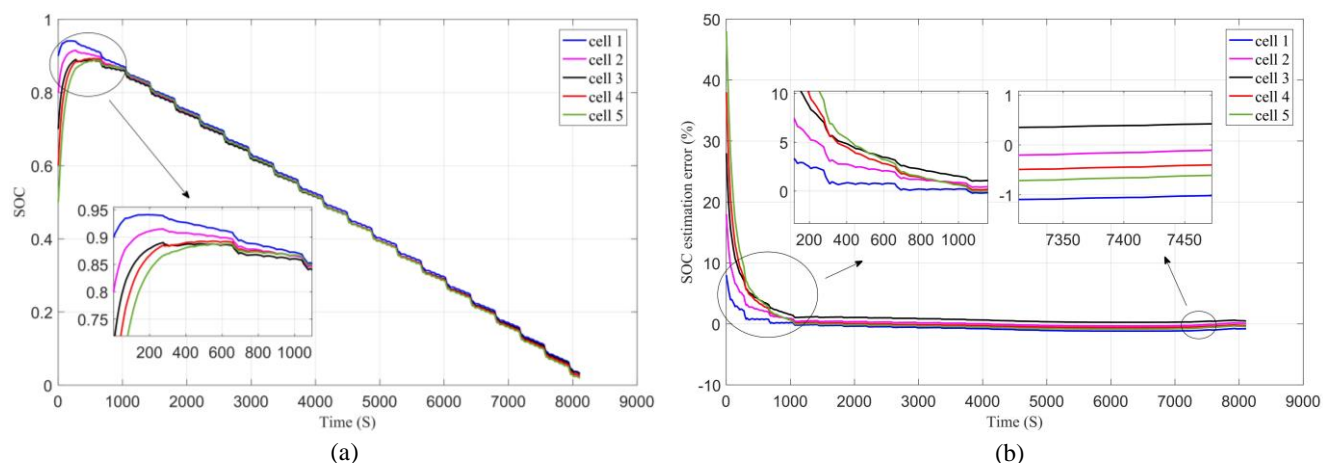


Figure 9. Verification of algorithm accuracy and robustness under DST conditions. (a) SOC estimation results with different initial errors of individual cells; (b) SOC estimation error changing with different initial errors

6. CONCLUSION

This paper starts with the analysis of battery cell differences, summarizes the battery inconsistency that affects the accuracy of battery pack’s cell SOC estimation, and determines the factors considered in this paper: voltage, ohmic resistance and capacity inconsistency. Then, the battery pack difference model is established based on the ECM, the selected cell corresponds to the second-order RC ECM, and the other cell models are simplified to an ECM that only includes ohmic internal resistance,

and the polarization voltage of the selected cell is used to compensate the estimated values of the terminal voltage of the remaining cells to reduce the error and reduce the computational complexity. Additionally, Dual-AEKF were used to estimate the SOC of the selected cell and the remaining cells respectively. Based on the above methods, DST, HPPC and EWC are used for experimental verification. The results show that, compared with the GM, the calculation time of TPM is significantly reduced under different dynamic conditions. In addition, the SOC estimation error of all cells is within 1.8%. Compared with TPM-NA, TPM can reduce the SOC estimation error and RMSE. The experimental verification also shows that TPM has better robustness. Under different SOC initial errors, the estimation results can converge quickly. However, this paper does not consider the high and low temperature conditions, which will be used as the content of future research.

In general, TPM can estimate the SOC of all cells in the battery pack with a small computational burden under the premise of ensuring the estimation accuracy of all battery cells. The results show that the estimation accuracy and robustness are good.

ACKNOWLEDGMENTS

This work was financially supported by Zhejiang market supervision bureau “chick eagle project” (CY2022362)fund.

References

1. X.G. Wu, M.Z. Li, J.Y. Du, and F.F. Hu, *Energy Rep.*, 8(2022)2262-2272.
2. Z.L. Wang, G.J. Feng, D. Zhen, F.S. Gu, and A. Ball, *Energy Rep.*,7(2021)5141.
3. L.C. Ren, G.R. Zhu, J.V. Wang, B.Y. Luo, and J.Q. Kang, *J. Power Sources*, 478(2020)228767.
4. I.O. Essiet, Y.X. Sun, *Energy Rep.*, 7(2021)4348-4359.
5. Y.J. Wang, J.Q. Tian, Z.D. Sun, L. Wang, R.L. Xu, M.C. Li, and Z.H. Chen, *Renewable Sustainable Energy Rev.*, 131(2020) 110015.
6. P. Shrivastava, T.K. Soon, M.Y.I.B. Idris, and S. Mekhilef, *Renewable Sustainable Energy Rev.*, 11(2019)109233.
7. Y.F. Guo, Z.H. Zhao, and L.M. Huang, *Energy Procedia*, 105(2017)4153.
8. M.S.H. Lipu, M.A. Hannan, A. Hussain, M.H. Saad, A. Ayob, and M.N. Uddin, *IEEE Trans. Ind. Appl.*, 55(2019)4225.
9. X.F. Wang, Q. Sun, X. Kou, W.T. Ma, H. Zhang, and R. Liu, *Energy*, 239 (2022)122406.
10. C. Ephrem, K. Phillip J, P. Matthias, and E. Ali, *J. Power Sources*, 400(2018)242.
11. Q. Wang, M. Ye, M. Wei, G.Q. Lian, and C.G. Wu, *Energy Rep.*, 7(2021)7323.
12. H. Chaoui, C.C. Ibe-Ekeocha, *IEEE Trans. Veh. Technol.*, 66(2017)8773.
13. Z. Chen, H.Q. Zhao, X. Shu, Y.J. Zhang, J.W. Shen, and Y.G. Lin, *J. Mol. Liq.*, 228(2021)120630.
14. L. Zhang, K. Li, D.J. Du, and C.B. Zhu, *IFAC-PapersOnLine*, 52(2019)256.
15. Z.W. Deng, X.S. Hu, X.K. Lin, Y.H. Che, L. Xu, and W.C. Guo, *Energy*, 205(2020)118000.
16. M.S.H. Lipu, M.A. Hannan, A. Hussain, A. Ayob, M.H.M. Saad, T.F. Karim, and D.N.T. How, *J. Cleaner Prod.*, 277(2020)124110.
17. L. Guo, J.Q. Li, and Z.J. Fu, *Energy Procedia*, 158(2019)2599.
18. S. Sepasi, R. Ghorbani, and B.Y. Liaw, *J. Power Sources*, 255(2014)368.
19. H.F. Dai, X.Z. Wei, Z.C. Sun, J.Y. Wang, and W.J. Gu, *Appl. Energy*, 95(2012)227.
20. J.K. Peng, J.Y. Luo, H.W. He, and B. Lu, *Appl. Energy*, 253(2019)113520.
21. S.Y. Fu, W. Liu, W.L. Luo, Z.F. Zhang, M.H. Zhang, L. Wu, C.D. Luo, T.L. Lv, and J.Y. Xie, *J.*

- Energy Storage*, 50(2022)104175.
22. J.Y. Luo, J.K. Peng, and H.W. He, *J Energy Procedia*, 158(2019)3421.
 23. T.C. Ouyang, P.H. Xu, J.X. Chen, J. Lu, and N. Chen, *Electrochim. Acta*, 353(2020) 136576.
 24. F.F. Yang, S.H. Zhang, W.H. Li, and Q. Miao, *Energy*, 201(2020)117664.
 25. S.M. Peng, X.L. Zhu, Y.J. Xing, H.B. Shi, X. Cai, and M. Pecht, *J. Power Sources*, 392(2018)48.
 26. J.H. Meng, G.Z. Luo, and F. Gao, *IEEE Trans. Power Electron.*, 31(2016)2226-2238.
 27. Z. Liu, X.J. Dang, B.Q. Jing, and J.B. Ji, *Electr. Power Syst. Res.*, 177(2019)105951.
 28. Z.G. He, Y.T. Li, Y.Y. Sun, S.C. Zhao, C.F. Pan, and L.M. Wang, *J. Energy Storage*, 39(2021)102593.
 29. H. Yang, X.Z. Sun, Y.B. An, X. Zhang, T.Z. Wei, and Y.W. Ma, *Int. J. Energy Res.*, 24(2019) 100810.
 30. Y. Tian, R.C. Lai, X.Y. Li, L.J. Xiang, and J.D. Tian, *Appl. Energy*, 265(2020)114789.
 31. C.F. Yang, X.Y. Wang, Q.H. Fang, H.F. Dai, Y.Q. Cao, and X.Z. Wei, *J. Energy Storage*, 29(2020)101250.
 32. Z.K. Zhou, B. Duan, Y.Z. Kang, N.X. Cui, Y.L. Shang, and C.H. Zhang, *J. Power Sources*, 441(2019)226972.
 33. L. Zhong, C.B. Zhang, Y. He, and Z.H. Chen, *Appl. Energy*, 113(2014)558-564.
 34. J.W. Wei, G.Z. Dong, Z.H. Chen, and Y. Kang, *Appl. Energy*, 187(2017)37-49.
 35. J.H. Li, B. Greye, M. Buchholz, and M.A. Danzer, *J. Power Sources*, 13(2017)1-9.
 36. R. Xiong, F.C. Sun, X.Z. Gong, and H.W. He, *J. Power Sources*, 242(2013)699-713.
 37. F. Feng, X.S. Hu, L. Hu, F.L. Hu, Y. Li, and L. Zhang, *Renewable Sustainable Energy Rev.*, 112(2019)102-113.
 38. B. Kenney, K. Darcovich, D.D. MacNeil, and I.J. Davidson, *J. Power Sources*, 213(2012)391-401.
 39. X.Z. Gong, R. Xiong, and C.C. Mi, *IEEE Trans. Ind. Appl.*, 51(2015) 1872-1879.
 40. Y.L. Zhang, J. Xu, S.C. Yang, C. Dong, F. Chen, and F. Lei, *Adv. Mech. Eng.*, 9(2017)1-13.
 41. Q.S. Wang, Z.P. Wang, L. Zhang, P. Liu, and Z.S. Zhang, *IEEE Trans. Transp. Electrifi.*, 7(2021)437-451.
 42. Y. Tian, Z.J. Huang, X.Y. Li, and J.D. Tian, *Energy*, 239(2022)122181.
 43. M.N. Ma, Q.L. Duan, C.P. Zhao, Q.S. Wang, and J.H. Sun, *IEEE Trans. Veh. Technol.*, 69(2020)10797-10808.
 44. A. Jokar, B. Rajabloo, M. Désilets, and M. Lacroix, *J. Power Sources*, 327(2016)44-55.
 45. X. Lai, Y.J. Zheng, and T. Sun, *Electrochim. Acta*, 259(2018)566-577.
 46. R.X. Xiao, Y.W. Hu, X.G. Jia, and G.S. Chen, *Energy*, 243(2022)123072.
 47. G. Li, D.Y. Zhao, R.C. Xie, H.L. Han, and C.F. Zong, *Rev. Automot. Eng.*, 12(2015)1426-1432.
 48. S. Nejad, D.T. Gladwin, and D.A. Stone, *J. Power Sources*, 316(2016)183-196.